J. Chem. Sci. Vol. 129, No. 7, July 2017, pp. 849–858. © Indian Academy of Sciences.
DOI 10.1007/s12039-017-1232-3

REGULAR ARTICLE

Special Issue on THEORETICAL CHEMISTRY/CHEMICAL DYNAMICS

Modeling of 1-D Nanowires and analyzing their Hydrogen and Noble Gas Binding Ability†

SUDIP PAN[a], RANAJIT SAHA[a], ASHUTOSH GUPTA[b] and PRATIM K CHATTARAJ[a,*]

[a]Department of Chemistry and Center for Theoretical Studies, Indian Institute of Technology Kharagpur, Kharagpur, West Bengal 721 302, India

[b]Department of Chemistry, Udai Pratap Autonomous College, Varanasi, Uttar Pradesh 221 005, India

Email: pkc@chem.iitkgp.ernet.in

MS received 14 November 2016; revised 2 January 2017; accepted 3 January 2017

Abstract. The theoretical calculation at the M05-2X/6-311+G(d,p) level reveals that the B–B bond length in $[N_4\text{-}B_2\text{-}N_4]^{2-}$ system (1.506 Å) is slightly smaller than that of typical B=B bond in B_2H_2 (1.518 Å). These systems interact with each M^+ (M = Li, Na, K) ion very strongly with a binding energy of 213.5 (Li), 195.2 (Na) and 180.3 (K) kcal/mol. Additionally, the relief of the Coulomb repulsion due to the presence of counter-ion, M^+, the B–B bond contracts to 1.484–1.488 Å in $[N_4\text{-}B_2\text{-}N_4]M_2$. We have further extended our study to $[N_4\text{-}B_2\text{-}N_4\text{-}B_2\text{-}N_4]^{4-}$ and $[N_4\text{-}B_2\text{-}N_4\text{-}B_2\text{-}N_4\text{-}B_2\text{-}N_4]^{6-}$ systems. The B–B bond length is found to be 1.496 Å in the former case, whereas the same is found to be 1.493 Å and 1.508 Å, respectively, for the two B–B bonds present in the latter one. The M^+ counter-ions stabilize such negatively charged systems and thus, create a possibility to design a long 1-D nanowire. Their utilities as probable hydrogen and noble gas (Ng) binding templates are explored taking $[N_4\text{-}B_2\text{-}N_4\text{-}B_2\text{-}N_4]Li_4$ system as a reference. It is found that each Li center binds with three H_2 molecules with an average binding energy of 2.1 kcal/mol, whereas each Ng (Ar–Rn) atom interacts with Li center having a binding energy of 1.8–2.1 kcal/mol. The H_2 molecules interact with Li centers mainly through equal contribution from orbital and electrostatic interaction, whereas the orbital interaction is found to be major term (*ca.* 51–58%) in Ng-Li interaction followed by dispersion (*ca.* 24–27%) and electrostatic interaction (*ca.* 17–24%).

Keywords. B–B multiple bond; hydrogen storage; noble gas binding; HOMO-LUMO energy gap.

1. Introduction

In recent time, the finding of multiple bonds between boron atoms is a hot topic of research.[1–3] A well-known concept in chemistry assigns the bond order of X-Y (X, Y = any p-block element) to be generally smaller than that dictated by their number of valence electrons. The concept seems to have broken down with the synthesis of a gallyne complex, $Na_2[Mes^*_2C_6H_3\text{-}GaGa\text{-}C_6H_3Mes^*_2]$ (Mes^* = 2,4,6-*i*-$Pr_3C_6H_2$)[4] and OCBBCO.[5] The theoretical calculation on LBBL (L = CO, N_2, CS)[6] and $[OBBBBO]^{2-}$ have revealed some degree of triple bond character in the B–B bonds present therein.[7] In 2011, the groups of Frenking[8] and Mitoraj[9] predicted *in silico* a viable bis(N-heterocyclic carbene) (NHC)-stabilized −B≡B− system which was isolated by Braunschweig and coworkers[10] in the very next year. Further, the replacement of 1,3-bis(2,6-diisopropylphenyl)imidazol-2-ylidene (IDip) of this compound by 3,3,5,5-tetramethyl-1-(2′, 6′-diisopropylphenyl)-pyrrolidine-2-ylidene (cAAC) causes slight elongation of the B–B bond and compression of the B–C bond.[11] The bonding situation in these compounds can be understood in terms of donor−acceptor type of interaction where the ligands act as donors and B_2 moiety acts as an acceptor. The B_2 fragment in this compound resides in its third excited $^1\sum_g^+$ state having valence electronic configuration $(2\sigma_g)^2(1\pi_u)^4$ making the formal bond order of three.[12]

The scarcity of systems having B–B multiple bonds is due to the electron deficient nature of boron. In the present study, we have shown that some degree of B–B triple bond character is present in $[N_4\text{-}B_2\text{-}N_4]^{2-}$. Further, we have extended our study to $[N_4\text{-}B_2\text{-}N_4\text{-}B_2\text{-}N_4]^{4-}$ and $[N_4\text{-}B_2\text{-}N_4\text{-}B_2\text{-}N_4\text{-}B_2\text{-}N_4]^{6-}$. We have included M^+ (M = Li, Na, K) as counter-ion to provide stability to these highly anionic systems. In this way, 1-D nanowires are modeled in which the cationic M centers can trap H_2 molecules and noble gas (Ng) atoms.

The use of hydrogen as an energy alternative to the fossil fuel is conceived due to some of its astonishing

*For correspondence

† Dedicated to the memory of the late Professor Charusita Chakravarty

merits,[13–15] *viz*., (i) its rank in abundance as the third in nature, (ii) the production of only environmentally clean water vapor upon combustion, (iii) the high energy density per unit mass, (iv) quick dissipating power of it minimizing accident due to its leakage, (v) its recyclability, and (vi) renewability. Hydrogen as a fuel, therefore, triggers the growth of a "clean energy economy" and a pollution-free environment. Now, for practical industrial and automobile applications, hydrogen needs to be stored in required gravimetric and volumetric quantities. Being a gas, hydrogen at normal conditions occupies a large volume. However, the liquefaction of hydrogen needs cryogenic temperature and high pressure, an extreme condition that can hardly be maintained for daily usage purposes. Therefore, the hunt of suitable hydrogen storing templates has turned out as a vastly cultivated topic. For the sake of reversibly storing and releasing of hydrogen at near ambient condition, the hydrogen binding energy should be in between that of physisorption and chemisorption where the hydrogen is stored mainly in molecular form.[16,17] Numerous varieties of molecular template materials like clathrate hydrates,[18,19] polymers,[20] alanates,[21] metal organic frameworks (MOF),[22,23] covalent organic frameworks (COF),[24,25] Li-decorated systems,[26–31] carbon nanotubes,[32,33] boron nanotubes,[34,35] fullerenes,[36,37] graphene-like materials,[38–41] BN cages,[42] metal hydrides[43] and metal borohydrides,[44] cucurbit-[n]urils[45] are theoretically designed and/or experimentally tested to afford a fruitful storage potential.

On the other hand, Ng-chemistry is one of the less explored fields because of the poor reactivity of Ng atoms, originated from its completely filled valence electronic shell. However, since the last two decades there has been a significant advancement as several Ng-compounds are either synthesized in crystal forms[46–55] or detected in the gas phase[56–61] or predicted theoretically.[62–92] The present investigation shows that the positively charged Li center can bind H_2 molecules with an average binding energy of 2.1–2.6 kcal/mol per H_2, whereas Ar–Rn atoms interact with Li center having a binding energy ranging from 1.8 to 2.1 kcal/mol. The variation of energy gap between the highest occupied molecular orbital (HOMO) and the lowest unoccupied molecular orbital (LUMO) with an increase in chain length is also studied for analyzing the probable use of it in the field of electronics.

2. Computational details

All the systems studied here are optimized at the M05-2X[93]/6-311+G(d,p)[94,95] level of theory using Gaussian 09 program package.[96] For the Ng-bound analogues, to include the relativistic effect we have used an effective core potential at the M05-2X/def2-TZVP[97] level. Effective core potential is used for Xe and Rn atoms. Harmonic vibrational frequency analysis is also performed for all the structures at the mentioned level to assess their existence as minima on the potential energy surface (PES). Natural population analysis (NPA)[98] is done to know the nature of bonding therein. The Wiberg bond index (WBI)[99] is also computed to assess the bond order. Average binding energy per H_2 molecule (E_b) is calculated by using eq. (1)

$$E_b = (1/n)\left[\left(E_{system} + nE_{H_2}\right) - E_{nH_2@system}\right] \quad (1)$$

The nature of interaction between H_2 or Ng and Li centers is also analyzed by energy decomposition analysis (EDA)[100] at the PBE-D3/TZ2P level by taking the optimized geometries at the aforementioned level using the ADF (2013.01) package.[101,102] Instead of frozen core approximation, an all-electron basis set was used. The interaction energy (ΔE_{int}) between two fragments is defined as:

$$\Delta E_{int} = \Delta E_{Pauli} + \Delta E_{elstat} + \Delta E_{orb} + \Delta E_{disp} \quad (2)$$

In EDA calculation, ΔE_{int} between two fragments is decomposed into four energy terms, *viz*., 1) electrostatic interaction energy (ΔE_{elstat}), which is classically calculated considering the charge distribution to be unperturbed on each fragment by other one; 2) Pauli repulsion (ΔE_{Pauli}), which appears as the repulsive energy between electrons of the same spin and it is computed by employing Kohn-Sham determinant on the superimposed fragments to obey the Pauli principle by anti-symmetrization and renormalization; 3) orbital interaction energy (ΔE_{orb}) that originates from the mixing of orbitals, charge transfer and polarization between two fragments in the compound; and 4) dispersion interaction energy (ΔE_{disp}), which represents the dispersion interaction occurring between the two fragments.

3. Results and Discussion

3.1 *B–B multiple bonds*

The energy minimum structures for $[N_4\text{-}B_2\text{-}N_4]^{2-}$, $[N_4\text{-}B_2\text{-}N_4\text{-}B_2\text{-}N_4]^{4-}$ and $[N_4\text{-}B_2\text{-}N_4\text{-}B_2\text{-}N_4\text{-}B_2\text{-}N_4]^{6-}$ are provided in Figure 1. The B–B bond distance in $[N_4\text{-}B_2\text{-}N_4]^{2-}$ system is 1.509 Å, whereas the same for $[N_4\text{-}B_2\text{-}N_4\text{-}B_2\text{-}N_4]^{4-}$ is 1.496 Å. $[N_4\text{-}B_2\text{-}N_4\text{-}B_2\text{-}N_4\text{-}B_2\text{-}N_4]^{6-}$ system has two types of B–B bonds having the bond distances of 1.493 Å and 1.508 Å, respectively. At the same level, the typical B=B and B≡B bond distances in B_2H_2 and $B_2H_2^{2-}$ are 1.518 Å and 1.494 Å, respectively. Further, the B–B bond distances in

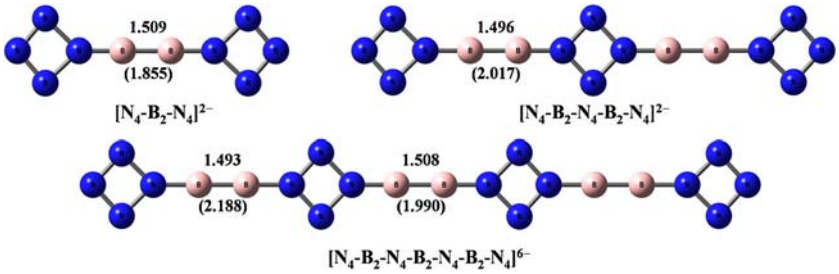

Figure 1. The optimized geometries of $[N_4\text{-}B_2\text{-}N_4]^{2-}$, $[N_4\text{-}B_2\text{-}N_4\text{-}B_2\text{-}N_4]^{4-}$, and $[N_4\text{-}B_2\text{-}N_4\text{-}B_2\text{-}N_4\text{-}B_2\text{-}N_4]^{6-}$ systems studied at the M05-2X/6-311+G(d,p) level. (The values without bracket show the B–B bond distances in Å unit and the values within bracket show the WBI of B–B bonds).

the reported OCBBCO, $[OBBBBO]^{2-}$, and N_2BBN_2 systems[5–7] are 1.430 Å, 1.472 Å and 1.421 Å, respectively, at the M05-2X/6-311+G(d,p) level. The WBI of B–B bonds in $[N_4\text{-}B_2\text{-}N_4]^{2-}$ and $[N_4\text{-}B_2\text{-}N_4\text{-}B_2\text{-}N_4]^{4-}$ are 1.855 and 2.017, respectively, whereas $[N_4\text{-}B_2\text{-}N_4\text{-}B_2\text{-}N_4\text{-}B_2\text{-}N_4]^{6-}$ has WBI values of 2.188 and 1.990 for its two types of B–B bonds. The values of WBI in our considered systems are very much comparable to those of the OCBBCO (WBI = 2.074) and N_2BBN_2 (WBI = 2.038). The B–B stretching frequency in $[N_4\text{-}B_2\text{-}N_4]^{2-}$ is 1807.6 cm^{-1}, which is slightly higher than those of the reported OCBBCO (1753.6 cm^{-1}), N_2BBN_2 (1774.4 cm^{-1}) and $[OBBBBO]^{2-}$ (1554.6 cm^{-1}) systems. Therefore, comparison of the B–B bond distances, WBI and B–B stretching frequencies of our studied systems with those of the reported systems reveals the existence of some degree of B≡B bonds in $[N_4\text{-}B_2\text{-}N_4]^{2-}$, $[N_4\text{-}B_2\text{-}N_4\text{-}B_2\text{-}N_4]^{4-}$, and $[N_4\text{-}B_2\text{-}N_4\text{-}B_2\text{-}N_4\text{-}B_2\text{-}N_4]^{6-}$.

3.2 *Stability in presence of counter-ions*

Although the absence of any imaginary frequency shows the existence of $[N_4\text{-}B_2\text{-}N_4]^{2-}$, $[N_4\text{-}B_2\text{-}N_4\text{-}B_2\text{-}N_4]^{4-}$, and $[N_4\text{-}B_2\text{-}N_4\text{-}B_2\text{-}N_4\text{-}B_2\text{-}N_4]^{6-}$ at minima on the respective potential energy surfaces, as such they only remain as hypothetical species since their HOMO and even lower lying electrons of these multi-anionic species are unbound in nature, showing their electronic instability with respect to spontaneous emission of electrons. Therefore, combination with proper number of counter-ions should be provided to make them viable. Here, we have considered M^+ (M = Li, Na, K) as counter-ions. Putting M^+ ions at different positions, a number of isomers for $[N_4\text{-}B_2\text{-}N_4]M_2$ are identified; however, the most stable isomers are given in Figure 2. Similarly, the optimized geometries of $[N_4\text{-}B_2\text{-}N_4\text{-}B_2\text{-}N_4]M_4$, $[N_4\text{-}B_2\text{-}N_4\text{-}B_2\text{-}N_4\text{-}B_2\text{-}N_4]M_6$ and $[N_4\text{-}B_2\text{-}N_4\text{-}B_2\text{-}N_4\text{-}B_2\text{-}N_4\text{-}B_2\text{-}N_4]M_8$ are also displayed in Figure 2. It is found that in the presence of M^+ ion, the planarity of the $-N_4\text{-}B_2\text{-}N_4-$ moiety gets lost and the N_4 rings bend towards the same direction of the location of M atoms to maximize the interaction between M and N_4 unit without affecting the interaction between M and B_2 unit. Consequently, with an increase in the chain length, beautiful zig-zag shaped structures result (Figure 2). Interestingly, in the absence of M, a free optimization starting from such bent geometry leads to the same planar structure which confirms that presence of M provides such zig-zag orientation in the $-N_4\text{-}B_2\text{-}N_4-$ moiety. Here, we have assessed the stability up to $[N_4\text{-}B_2\text{-}N_4\text{-}B_2\text{-}N_4\text{-}B_2\text{-}N_4\text{-}B_2\text{-}N_4]M_8$ and it is expected that in this way one can design a long 1-D nanowire.

The B–B bond distances (d_{B-B}) in presence of M^+ counter-ions get shortened to 1.479–1.492 Å with respect to those in anionic systems, due to the reduction of coulomb repulsion in the neutral systems. In $[N_4\text{-}B_2\text{-}N_4\text{-}B_2\text{-}N_4]Li_4$, d_{B-B} is 1.481 Å, whereas in $[N_4\text{-}B_2\text{-}N_4\text{-}B_2\text{-}N_4]^{4-}$, it is 1.496 Å. Note that there is no correlation between WBI and d_{B-B}, which was also previously pointed out by Frenking *et al.*,[6] in their studied systems. Now, since M centers in these systems possess large positive charges ($\approx +0.8\ |e|$), they may behave as active centers in binding H_2 molecules and Ng atoms.

3.3 *Interaction with hydrogen molecules and noble gas*

Taking $[N_4\text{-}B_2\text{-}N_4\text{-}B_2\text{-}N_4]M_4$ as an example, we have explored the H_2 binding ability of each M center. Na and K have very low H_2 binding ability compared to Li because of lower ionic potential of the former ones than the latter one. Therefore, we have discussed only the results for Li analogue. Each Li center is found to bind with maximum three H_2 molecules, so a total of 12 H_2 molecules interact with $[N_4\text{-}B_2\text{-}N_4\text{-}B_2\text{-}N_4]Li_4$ (Figure 3). Each H_2 in $12H_2@[N_4\text{-}B_2\text{-}N_4\text{-}B_2\text{-}N_4]Li_4$ interacts with Li center having binding energy of 2.1 kcal/mol (Table 1). The correction to D_0 from the basis set superposition error (BSSE) as computed by the standard counterpoise method of Boys and Bernardi[103]

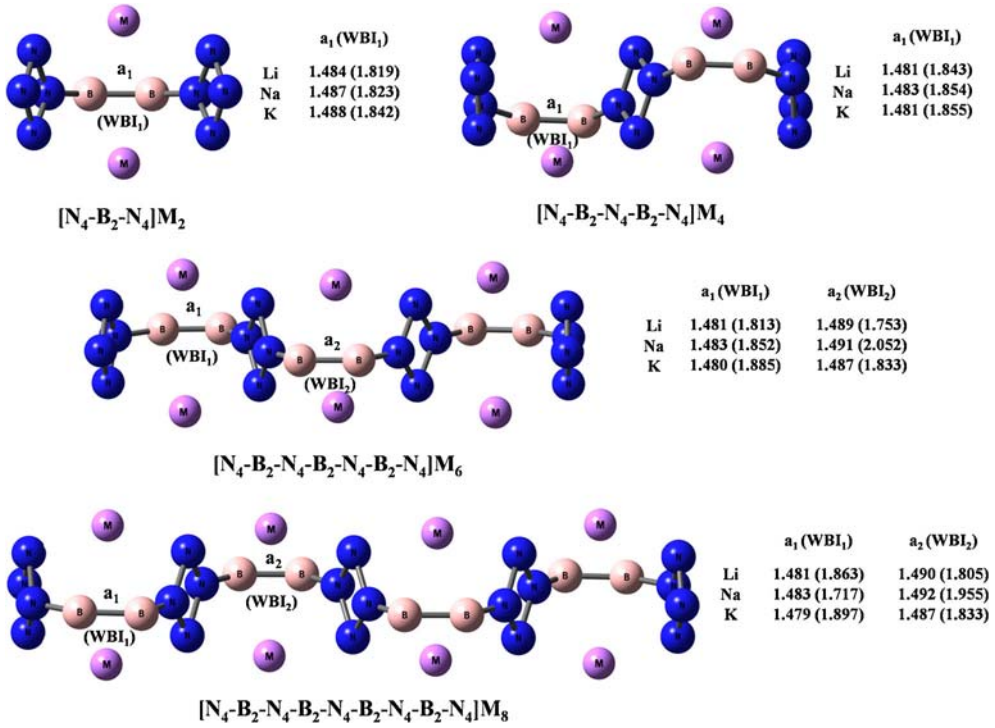

Figure 2. The optimized geometries of $[N_4\text{-}B_2\text{-}N_4]Li_2$, $[N_4\text{-}B_2\text{-}N_4\text{-}B_2\text{-}N_4]Li_4$, $[N_4\text{-}B_2\text{-}N_4\text{-}B_2\text{-}N_4\text{-}B_2\text{-}N_4]Li_6$ and $[N_4\text{-}B_2\text{-}N_4\text{-}B_2\text{-}N_4\text{-}B_2\text{-}N_4\text{-}B_2\text{-}N_4]Li_8$ studied at the M05-2X/6-311+G(d,p) level.

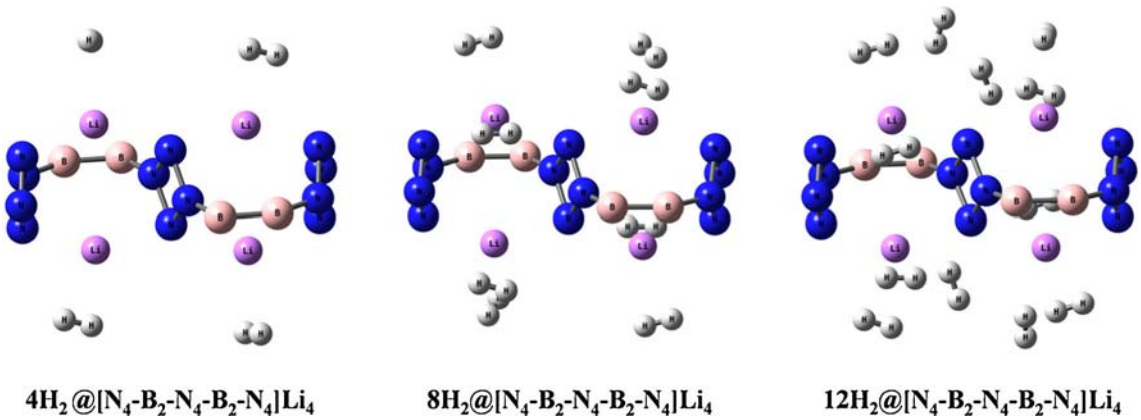

Figure 3. The optimized geometries of $nH_2@[N_4\text{-}B_2\text{-}N_4\text{-}B_2\text{-}N_4]Li_4$ (n = 4, 8 and 12) studied at the M05-2X/6-311+G(d,p) level.

Table 1. The binding energy (E_b, kcal/mol) per H_2 molecule, dissociation enthalpy at 298K (ΔH, kcal/mol) for the process $nH_2@[N_4\text{-}B_2\text{-}N_4\text{-}B_2\text{-}N_4]Li_4 \rightarrow nH_2 + [N_4\text{-}B_2\text{-}N_4\text{-}B_2\text{-}N_4]Li_4$, charge at Li center ($Q_{Li}$, |*e*|), B–B bond distance (d_{B-B}, Å) and Wiberg bond index (WBI_{B-B}) of B–B bonds studied at the M05-2X/6-311+G(d,p) level.

Systems	E_b	ΔH	Q_{Li}	d_{B-B}	WBI_{B-B}
$[N_4\text{-}B_2\text{-}N_4\text{-}B_2\text{-}N_4]Li_4$			+0.76	1.481	1.806
$4H_2@[N_4\text{-}B_2\text{-}N_4\text{-}B_2\text{-}N_4]Li_4$	2.4	3.0	+0.66	1.481	1.780
$8H_2@[N_4\text{-}B_2\text{-}N_4\text{-}B_2\text{-}N_4]Li_4$	2.6	7.8	+0.56	1.480, 1.481	1.760, 1.761
$12H_2@[N_4\text{-}B_2\text{-}N_4\text{-}B_2\text{-}N_4]Li_4$	2.1	6.9	+0.55–0.57	1.480	1.759

is negligible. For example, in $12H_2$ bound analogue the BSSE corrected binding energy is 2.0 kcal/mol per H_2 molecule. The dissociation enthalpy values for all H_2 binding processes are also endothermic in nature. Upon the inclusion of H_2 molecules, d_{B-B} values remain almost unchanged. The positive charge on Li center gradually decreases with the number of bound H_2 showing some degree of electron transfer from H_2 molecule to Li center. The HOMO-LUMO energy gap, which is also a measure of chemical hardness,[104–107] is 5.52 eV for $[N_4\text{-}B_2\text{-}N_4]Li_2$, 5.23 eV for $[N_4\text{-}B_2\text{-}N_4\text{-}B_2\text{-}N_4]Li_4$, 4.87 eV for $[N_4\text{-}B_2\text{-}N_4\text{-}B_2\text{-}N_4\text{-}B_2\text{-}N_4]Li_6$ and 4.72 eV for $[N_4\text{-}B_2\text{-}N_4\text{-}B_2\text{-}N_4\text{-}B_2\text{-}N_4\text{-}B_2\text{-}N_4]Li_8$, respectively. It is interesting to note that the HOMO-LUMO energy gap gradually decreases with an increase in the chain length which hints at that in a material scale it would possess a wide-band gap and consequently these systems will show interesting optical and semiconductor properties.

Further, we have tested their Ng binding ability taking single Ng adsorption process on $[N_4\text{-}B_2\text{-}N_4\text{-}B_2\text{-}N_4]Li_4$ as a reference (Figure 4). The Li–Ng bond dissociation energy values in all cases are positive ranging from 1.8 to 2.1 kcal/mol which shows the bound nature of Ng atoms (Table 2). The Ng-dissociation processes are endothermic in nature at 298 K within the range of 1.4–1.7 kcal/mol. Upon binding, the positive charge on Li center decreases and positive charges are developed on Ng centers. It indicates some degree of electron transfer from Ng atoms to Li centers. The WBI values for Li–Ng bonds vary from 0.15 to 0.22 with a gradual increase from Ar to Rn.

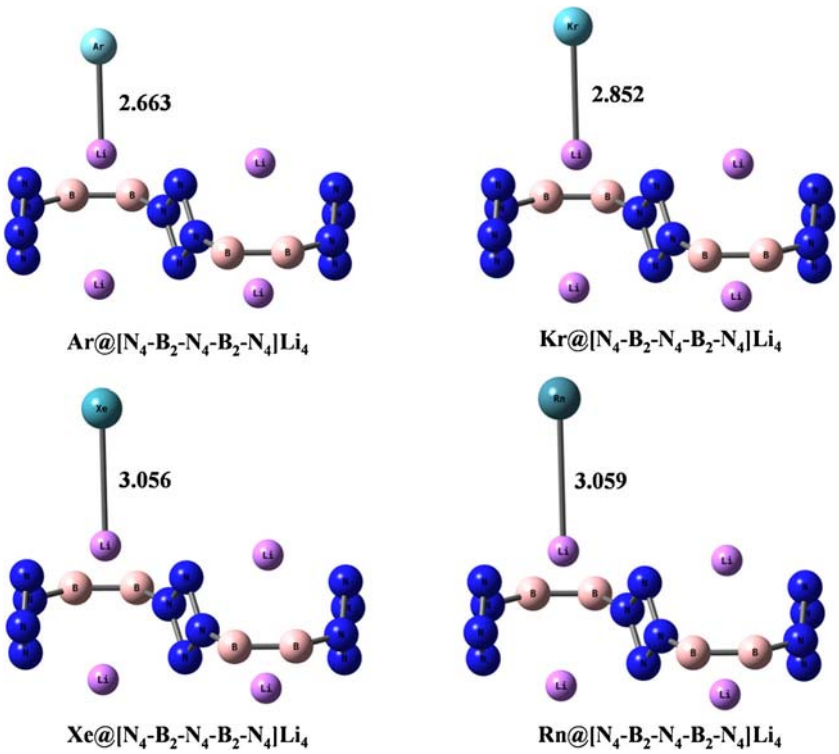

Figure 4. The optimized geometries of $Ng@[N_4\text{-}B_2\text{-}N_4]Li_2$ (Ng = Ar–Rn) studied at the M05-2X/def2-TZVP level.

Table 2. The binding energy (E_b, kcal/mol), dissociation enthalpy (ΔH, kcal/mol) at 298K for the process: $Ng@[N_4\text{-}B_2\text{-}N_4\text{-}B_2\text{-}N_4]Li_4 \rightarrow Ng + [N_4\text{-}B_2\text{-}N_4\text{-}B_2\text{-}N_4]Li_4$, charge at Li and Ng centers (Q, $|e|$), Li–Ng bond distance (d_{Li-Ng}, Å) and Wiberg bond index (WBI_{Li-Ng}) studied at the M05-2X/def2-TZVP level.

Systems	E_b	ΔH	Q_{Li}	Q_{Ng}	d_{Li-Ng}	WBI_{Li-Ng}
$[N_4\text{-}B_2\text{-}N_4\text{-}B_2\text{-}N_4]Li_4$			0.77			
$Ar@[N_4\text{-}B_2\text{-}N_4\text{-}B_2\text{-}N_4]Li_4$	1.8	1.4	0.64	0.08	2.663	0.149
$Kr@[N_4\text{-}B_2\text{-}N_4\text{-}B_2\text{-}N_4]Li_4$	1.9	1.5	0.62	0.09	2.852	0.171
$Xe@[N_4\text{-}B_2\text{-}N_4\text{-}B_2\text{-}N_4]Li_4$	1.8	1.5	0.60	0.11	3.056	0.200
$Rn@[N_4\text{-}B_2\text{-}N_4\text{-}B_2\text{-}N_4]Li_4$	2.1	1.7	0.59	0.12	3.059	0.216

Table 3. EDA results for the binding of $[N_4\text{-}B_2\text{-}N_4\text{-}B_2\text{-}N_4]Li_4$ with nH_2 (n = 4, 8,12) and Ng (Ng = Ar–Rn) at the PBE-D3/TZ2P level.

Systems	ΔE_{Pauli}	ΔE_{elstat}	ΔE_{orb}	ΔE_{disp}	ΔE_{int}
$4H_2@[N_4\text{-}B_2\text{-}N_4\text{-}B_2\text{-}N_4]Li_4$	2.8	−2.5 (46.1)	−2.3 (43.3)	−0.6 (10.6)	−2.6
$8H_2@[N_4\text{-}B_2\text{-}N_4\text{-}B_2\text{-}N_4]Li_4$	3.3	−2.8 (46.6)	−2.4 (40.1)	−0.8 (13.2)	−2.7
$12H_2@[N_4\text{-}B_2\text{-}N_4\text{-}B_2\text{-}N_4]Li_4$	2.9	−2.3 (45.6)	−2.0 (39.1)	−0.8 (15.3)	−2.3
$Ar@[N_4\text{-}B_2\text{-}N_4\text{-}B_2\text{-}N_4]Li_4$	1.9	−1.0 (24.3)	−2.0 (51.7)	−0.9 (24.0)	−2.0
$Kr@[N_4\text{-}B_2\text{-}N_4\text{-}B_2\text{-}N_4]Li_4$	1.6	−0.7 (17.0)	−2.3 (55.7)	−1.1 (27.3)	−2.5
$Xe@[N_4\text{-}B_2\text{-}N_4\text{-}B_2\text{-}N_4]Li_4$	2.0	−0.9 (17.1)	−2.9 (58.2)	−1.2 (24.7)	−3.1
$Rn@[N_4\text{-}B_2\text{-}N_4\text{-}B_2\text{-}N_4]Li_4$	3.0	−1.4 (21.9)	−3.3 (53.4)	−1.5 (24.8)	−3.2

The values within the parentheses are in percentage and show the contribution towards the total attractive interaction $\Delta E_{elstat} + \Delta E_{orb} + \Delta E_{disp}$.

3.4 *Energy decomposition analysis*

The EDA calculations[108–114] were carried out to shed light into the nature of interaction between $[N_4\text{-}B_2\text{-}N_4\text{-}B_2\text{-}N_4]Li_4$ and H_2 or Ng in their corresponding H_2 or Ng bound analogues, considering nH_2 or Ng as one fragment and $[N_4\text{-}B_2\text{-}N_4\text{-}B_2\text{-}N_4]Li_4$ as another (see Table 3). For H_2 bound systems, the corresponding energy values per H_2 molecule show that the contribution from ΔE_{elstat}(*ca.* 45–47%) is slightly larger than that from ΔE_{orb}(*ca.* 39–43%). ΔE_{elstat} and ΔE_{orb} are responsible for 84–90% of total attraction, whereas only 10–16% of the total attractive energy arises from the ΔE_{disp} term. On the other hand, in case of Ng bound complexes, the Ng–Li contacts are supported dominantly by the orbital interaction (*ca.* 51–58%), whereas the contribution from ΔE_{disp} (*ca.* 24–27%) is larger than that from ΔE_{elstat} (*ca.* 17–24%). In other words, while the interaction between Li center and H_2 is arisen from the almost equal orbital and electrostatic contributions, the Ng–Li bonds possess larger orbital interaction than ionic and dispersion interactions.

4. Conclusions

The B–B bonds in $[N_4\text{-}B_2\text{-}N_4]^{2-}$, $[N_4\text{-}B_2\text{-}N_4\text{-}B_2\text{-}N_4]^{4-}$, and $[N_4\text{-}B_2\text{-}N_4\text{-}B_2\text{-}N_4\text{-}B_2\text{-}N_4]^{6-}$ systems possess some degree of triple bond character. The electronic stability of these highly anionic systems can be provided by combining with an adequate number of M^+ (M = Li, Na, K) ions. Here, we have tested the stability up to $[N_4\text{-}B_2\text{-}N_4\text{-}B_2\text{-}N_4\text{-}B_2\text{-}N_4\text{-}B_2\text{-}N_4]Li_8$. But one can design a long chain of 1-D nanowire by linking N_4 rings through B_2 units and having a proper number of M^+ ions. Owing to a large positive charge on Li center, it can bind H_2 molecules and Ng atoms. Each Li center in $[N_4\text{-}B_2\text{-}N_4\text{-}B_2\text{-}N_4]Li_4$ can bind three H_2 molecules. The positive values of binding energy (within the range of 1.8–2.1 kcal/mol per H_2 or Ng) and endothermic nature of the associated dissociation processes predict their efficacy in binding H_2 and Ng. Some degree of electron transfer from H_2 and Ng to Li center plays crucial role in binding. Energy decomposition analysis reveals that the interaction between H_2 molecules and Li arises from the almost equal contributions from orbital and electrostatic interactions, whereas the orbital interaction plays a major role in Ng–Li interaction. The variation of energy gap between the highest occupied molecular orbital and the lowest unoccupied molecular orbital with an increase in chain length is noted to provide an insight into their possible application in the field of electronics.

Acknowledgements

This article is dedicated to the memory of the late Professor Charusita Chakravarty. P K Chattaraj thanks the Guest Editors for kindly inviting him to contribute an article in this Special Issue in honour of Professor Charusita Chakravarty. He would like to thank DST, New Delhi for the J. C. Bose National Fellowship. RS thanks UGC, New Delhi for his fellowship.

References

1. Moezzi A, Olmstead M M and Power P P 1992 Boron-boron double bonding in the species $[B_2R_4]^{2-}$: Synthesis and structure of $[\{(Et_2O)Li\}_2\{Mes_2BB(Mes)Ph\}]$, a diborane(4) dianion analog of a substituted ethylene *J. Am. Chem. Soc.* **114** 2715
2. Wang Y, Quillian B, Wei P, Wannere C S, Xie Y, King R B, Schaefer H F III, Schleyer P v R and Robinson G H 2007 A stable silicon (0) compound with a Si=Si double bond *J. Am. Chem. Soc.* **129** 12412
3. Braunschweig H and Dewhurst R D 2014 Boron–boron multiple bonding: From charged to neutral and back again *Organometallics* **33** 6271
4. Su J, Li X-W, Crittendon R C and Robinson G H 1997 How short is a −Ga≡Ga- triple bond? Synthesis

and molecular structure of $Na_2[Mes^*_2C_6H_3\text{-}Ga{\equiv}Ga\text{-}C_6H_3Mes^*_2]$($Mes^*$=2,4,6-*i*-$Pr_3C_6H_2$): The first gallyne *J. Am. Chem. Soc.* **119** 5471

5. Zhou M, Tsumori N, Li Z, Fan K, Andrews L and Xu Q 2002 OCBBCO: A neutral molecule with some boron-boron triple bond character *J. Am. Chem. Soc.* **124** 12936
6. Ducati L C, Takagi N and Frenking G 2009 Molecules with All Triple Bonds: OCBBCO, N_2BBN_2, and $[OBBBBO]^{2-}$ *J. Phys. Chem. A* **113** 11693
7. Li S-D, Zhai H-J and Wang L-S 2008 $B_2(BO)_2^{2-}$ diboronyl diborene: A linear molecule with a triple boron-boron bond *J. Am. Chem. Soc.* **130** 2573
8. Holzmann N, Stasch A, Jones C and Frenking G 2011 Structures and stabilities of group 13 adducts $[(NHC)(EX_3)]$ and $[(NHC)_2(E_2X_n)]$(E = B to In; X = H, Cl; n = 4, 2, 0; NHC = N-heterocyclic carbene) and the search for hydrogen storage systems: A theoretical study *Chem. Eur. J.* **17** 13517
9. Mitoraj M P and Michalak A 2011 Multiple boron-boron bonds in neutral molecules: An insight from the extended transition state method and the natural orbitals for chemical valence scheme *Inorg. Chem.* **50** 2168
10. Braunschweig H, Dewhurst R D, Hammond K, Mies J, Radacki K and Vargas A 2012 Ambient-temperature isolation of a compound with a boron-boron triple bond *Science* **336** 1420
11. Bçhnke J, Braunschweig H, Ewing W C, Hçrl C, Kramer T, Krummenacher I, Mies J and Vargas A 2014 Diborabutatriene: An electron-deficient cumulene *Angew. Chem. Int. Ed.* **53** 9082
12. Frenking G and Holzmann N 2012 A boron-boron triple bond *Science* **336** 1394
13. Schlapbach L and Züttel A 2001 Hydrogen-storage materials for mobile applications *Nature* **414** 353
14. Lubitz W and Tumas W 2007 Hydrogen: An overview *Chem. Rev.* **107** 3900
15. Chakraborty A, Duley S and Chattaraj P K 2012 Hydrogen storage: An overview with current insights based on a conceptual DFT approach *Indian J. Chem.* **51A** 226
16. Christian M L and Aguey-Zinsou K-F 2012 Core–shell strategy leading to high reversible hydrogen storage capacity for $NaBH_4$ *ACS Nano* **6** 7739
17. Yan Y, Remhof A, Rentsch D, Züttel A, Giri S and Jena P 2015 A novel strategy for reversible hydrogen storage in $Ca(BH_4)_2$ *Chem. Commun.* **51** 11008
18. Lee H, Lee J-W, Kim D Y, Park J, Seo Y-T, Zeng H, Moudrakovski I L, Ratcliffe C I and Ripmeester J A 2005 Tuning clathrate hydrates for hydrogen storage *Nature* **434** 743
19. Chattaraj P K, Bandaru S and Mondal S 2011 Hydrogen storage in clathrate hydrates *J. Phys. Chem. A* **115** 187
20. McKeown N B, Gahnem B, Msayib K J, Budd P M, Tattershall C E, Mahmood K, Tan S, Book D, Langmi H W and Walton A 2006 Towards polymer-based hydrogen storage materials: Engineering ultramicroporous cavities within polymers of intrinsic microporosity *Angew. Chem., Int. Ed.* **118** 1836
21. Baldé C P, Hereijgers B P C, Bitter J H and de Jong K P 2006 Facilitated hydrogen storage in $NaAlH_4$ supported on carbon nanofibers *Angew. Chem. Int. Ed.* **45** 3501
22. Rosi N L, Eckert J, Eddaoudi M, Vodak D T, Kim J, O'keeffe M and Yaghi O M 2003 Hydrogen storage in microporous metal-organic frameworks *Science* **300** 1127
23. Rowsel J L C and Yaghi O M 2005 Strategies for hydrogen storage in metal-organic frameworks *Angew. Chem. Int. Ed.* **44** 4670
24. Cabria I, López M J and Alonso J A 2008 Hydrogen storage capacities of nanoporous carbon calculated by density functional and Møller-Plesset methods *Phys. Rev. B*: *Condens. Matter Mater. Phys.* **78** 075415
25. Kuc A, Zhechkov L, Patchkovskii S, Seifert G and Heine T 2007 Hydrogen sieving and storage in fullerene intercalated graphite *Nano Lett.* **7** 1
26. Wu X, Gao Y and Zeng X C 2008 Hydrogen sieving and storage in fullerene intercalated graphite *J. Phys. Chem. C* **112** 8459
27. Er S, de Wijs G A and Brocks G 2009 DFT study of planar boron sheets: A new template for hydrogen storage *J. Phys. Chem. C* **113** 18962
28. Srinivasu K and Ghosh S K 2011 Theoretical studies on hydrogen adsorption properties of lithium decorated diborene ($B_2H_4Li_2$) and diboryne ($B_2H_2Li_2$) *Int. J. Hydrogen Energy* **36** 15681
29. Pan S, Giri S and Chattaraj P K 2012 A computational study on the hydrogen adsorption capacity of various lithium-doped boron hydrides *J. Comp. Chem.* **33** 425
30. Pan S, Banerjee S and Chattaraj P K 2012 Role of lithium decoration on hydrogen storage potential *J. Mex. Chem. Soc.* **56** 229
31. Pan S, Merino G and Chattaraj P K 2012 The hydrogen trapping potential of some Li-doped star-like clusters and super-alkali systems *Phys. Chem. Chem. Phys.* **14** 10345
32. Assfour B, Leoni S, Seifert G and Baburin I A 2011 Packings of carbon nanotubes–new materials for hydrogen storage *Adv. Mater.* **23** 1237
33. Liu C, Chen Y, Wu C-Z, Xu S-T and Cheng H-M 2010 Hydrogen storage in carbon nanotubes revisited *Carbon* **48** 452
34. Oku T 2014 Hydrogen storage in boron nitride and carbon nanomaterials *Energies* **8** 319
35. Mpourmpakis G and Froudakis G E 2007 Why boron nitride nanotubes are preferable to carbon nanotubes for hydrogen storage? An ab initio theoretical study *Catal. Today* **120** 341
36. Yoon M, Yang S, Hicke C, Wang E, Geohegan D and Zhang Z 2008 Calcium as the superior coating metal in functionalization of carbon fullerenes for high-capacity hydrogen storage *Phys. Rev. Lett.* **100** 206806
37. Wang Q, Sun Q, Jena P and Kawazoe Y 2009 Theoretical study of hydrogen storage in Ca-coated fullerenes *J. Chem. Theory Comput.* **5** 374
38. Ataca C, Aktürk E, Ciraci S and Ustunel H 2008 High-capacity hydrogen storage by metallized grapheme *Appl. Phys. Lett.* **93** 043123
39. Dimitrakakis G K, Tylianakis E and Froudakis G E 2008 Pillared graphene: A new 3-D network nanostructure for enhanced hydrogen storage *Nano Lett.* **8** 3166
40. Tozzini V and Pellegrini V 2013 Prospects for hydrogen storage in grapheme *Phys. Chem. Chem. Phys.* **15** 80
41. Shevlin S A and Guo Z X 2007 Hydrogen sorption in defective hexagonal BN sheets and BN nanotubes *Phys. Rev. B* **76** 024104

42. Sun Q, Wang Q and Jena P 2005 Storage of molecular hydrogen in BN cage: Energetics and thermal stability *Nano Lett.* **5** 1273
43. Lee H, Lee J-W, Kim D Y, Park J, Seo Y-T, Zeng H, Moudrakovski I L, Ratcliffe C I and Ripmeester J A 2005 Tuning clathrate hydrates for hydrogen storage *Nature* **434** 743
44. Kojima Y, Suzuki K-I, Fukumoto K, Sasaki M, Yamamoto T, Kawai Y and Hayashi H 2002 Hydrogen generation using sodium borohydride solution and metal catalyst coated on metal oxide *Int. J. Hydrogen Energy* **27** 1029
45. Pan S, Mondal S and Chattaraj P K 2013 Cucurbiturils as promising hydrogen storage materials: A case study of cucurbit [7] uril *New J. Chem.* **37** 2492
46. Hoppe R, Daehne W, Mattauch H and Roedder K 1962 Fluorination of xenon *Angew. Chem., Int. Ed. Engl.* **1** 599
47. Claassen H H, Selig H and Malm J G 1962 Xenon tetrafluoride *J. Am. Chem. Soc.* **84** 3593
48. Fields P R, Stein L and Zirin M H 1962 Radon fluoride *J. Am. Chem. Soc.* **84** 4164
49. Turner J J and Pinetel G C 1963 Krypton fluoride: Preparation by the matrix isolation technique *Science* **140** 974
50. Bartlett N, Wechsberg M, Jones G R and Burbank R D 1972 Crystal structure of xenon (II) fluoride fluorosulfate, $FXeOSO_2F$ *Inorg. Chem.* **11** 1124
51. Templeton L K, Templeton D H, Seppelt K and Bartlett N 1976 Crystal structure of $Xe(OSeF_5)_2$ *Inorg. Chem.* **15** 2718
52. Lentz D and Seppelt K 1979 $Xe(OTeF_5)_6$, a deep-colored noble gas compound, and $O{=}Xe(OTeF_5)_4$-the existence of $Kr(OTeF_5)_2$ *Angew. Chem., Int. Ed. Engl.* **18** 66
53. Schrobilgen G J, LeBlond N and Dixon D A 2000 Fluoride ion donor properties of TcO_2F_3 and ReO_2F_3: X-ray crystal structures of $MO_2F_3{\cdot}SbF_5$ (M = Tc, Re) and $TcO_2F_3{\cdot}XeO_2F_2$ and raman and NMR spectroscopic characterization of $MO_2F_3{\cdot}PnF_5$ (Pn = As, Sb), $[ReO_2F_2(CH_3CN)_2][SbF_6]$, and $[Re_2O_4F_5][Sb_2F_{11}]$ *Inorg. Chem* **39** 2473
54. Moran M D, Brock D S, Mercier H P A and Schrobilgen G J 2010 $Xe_3OF_3^+$, a precursor to a noble-gas nitrate; syntheses and structural characterizations of $FXeONO_2$, $XeF_2{\cdot}HNO_3$, and $XeF_2{\cdot}N_2O_4$ *J. Am. Chem. Soc.* **132** 13823
55. Bilir V, BaÈlser D, Boese R and Frohn H-J 2009 Bis(pentafluorophenylxenonium) tetrafluoroterephthalate, p-$C_6F_5XeO(O)CC_6F_4C(O)OXeC_6F_5$, a hypervalent compound with two xenon–carbon bonds *J. Fluorine Chem.* **130** 824
56. Thompson C A and Andrews L 1994 Noble gas complexes with BeO: Infrared spectra of NG–BeO (NG = Ar, Kr, Xe) *J. Am. Chem. Soc.* **116** 423
57. Feldman V I, Sukhov F F and Orlov A Y 1997 Further evidence for formation of xenon dihydride from neutral hydrogen atoms: A comparison of ESR and IR spectroscopic results *Chem. Phys. Lett.* **280** 507
58. Pettersson M, Lundell J, Khriachtchev L, Isamieni L and Räsänen M 1998 HXeSH, the first example of a xenon-sulfur bond *J. Am. Chem. Soc.* **120** 7979
59. Khriachtchev L, Pettersson M, Lundell J, Tanskanen H, Kiviniemi T, Runeberg N and Räsänen M 2003 A neutral xenon-containing radical, HXeO *J. Am. Chem. Soc.* **125** 1454
60. Cooke S A and Gerry M C L 2004 XeAuF *J. Am. Chem. Soc.* **126** 17000
61. Brock D S, Mercier H P A and Schrobilgen G J 2013 $[H(OXeF_2)_n][AsF_6]$ and $[FXe^{II}(OXe^{IV}F_2)_n][AsF_6]$($n$ = 1, 2): Examples of xenon(IV) hydroxide fluoride and oxide fluoride cations and the crystal structures of $[F_3Xe{-}FH][Sb_2F_{11}]$ and $[H_5F_4][SbF_6]{\cdot}2[F_3Xe{-}FH][Sb_2F_{11}]$ *J. Am. Chem. Soc.* **135** 5089
62. Koch W, Liu B and Frenking G 1990 Theoretical investigations of small multiply charged cations. III. NeN^{2+} *J. Chem. Phys.* **92** 2464
63. Frenking G, Koch W, Reichel F and Cremer D 1990 Light noble gas chemistry: Structures, stabilities, and bonding of helium, neon, and argon compounds *J. Am. Chem. Soc.* **112** 4240
64. Pan S, Gupta A, Mandal S, Moreno D, Merino G and Chattaraj P K 2015 Metastable behavior of noble gas inserted tin and lead fluorides *Phys. Chem. Chem. Phys.* **17** 972
65. Saha R, Pan S, Merino G and Chattaraj P K 2015 Comparative study on the noble-gas binding ability of BeX clusters (X = SO_4, CO_3, O) *J. Phys. Chem. A* **119** 6746
66. Lundell J, Cohen A and Gerber R B 2002 Quantum chemical calculations on novel molecules from xenon insertion into hydrocarbons *J. Phys. Chem. A* **106** 11950
67. Grochala W A 2012 A metastable He–O bond inside a ferroelectric molecular cavity: $(HeO)(LiF)_2$ *Phys. Chem. Chem. Phys.* **14** 14860
68. Frenking G, Koch W, Cremer D, Gauss J and Liebman J F 1989 Helium bonding in singly and doubly charged first-row diatomic cations $HeXn^+$ (X = Li–Ne; n = 1, 2) *J. Phys. Chem.* **93** 3397
69. Pan S, Moreno D, Cabellos J L, Romero J, Reyes A, Merino G and Chattaraj P K 2014 In quest of strong Be–Ng bonds among the neutral Ng–Be complexes *J. Phys. Chem. A* **118** 487
70. Khriachtchev L and Gerber R B 2009 Noble-gas hydrides: New chemistry at low temperatures *Acc. Chem. Res.* **42** 183
71. Frenking G, Gauss W J and Cremer D 1988 Stabilities and nature of the attractive interactions in HeBeO, NeBeO, and ArBeO and a comparison with analogs NGLiF, NGBN, and NGLiH (NG = He, Ar). A theoretical investigation *J. Am. Chem. Soc.* **110** 8007
72. Ghosh A, Dey S, Manna D and Ghanty T K 2015 Noble-gas-inserted fluoro (sulphido) boron (FNgBS, Ng = Ar, Kr, and Xe): A theoretical prediction *J. Phys. Chem. A* **119** 5732
73. Jayasekharan T and Ghanty T K 2008 Theoretical prediction of $HRgCO^+$ ion (Rg = He, Ne, Ar, Kr, and Xe) *J. Chem. Phys.* **129** 184302
74. Pan S, Saha R, Mandal S and Chattaraj P K 2016 σ-aromatic cyclic M_3^+ (M = Cu, Ag, Au) clusters and their complexation with dimethyl imidazol-2-ylidene, pyridine, isoxazole, furan, noble gases and carbon monoxide *Phys. Chem. Chem. Phys.* **18** 11661
75. Pan S, Saha R, Kumar A, Gupta A, Merino G and Chattaraj P K 2016 A noble interaction: An assessment of noble gas binding ability of metal oxides (metal = Cu, Ag, Au) *Int. J. Quantum Chem.* **116** 1016

76. Ghara M, Pan S, Kumar A, Merino G and Chattaraj P K 2016 Structure, stability, and nature of bonding in carbon monoxide bound EX_3^+ complexes (E = group 14 element; X = H, F, Cl, Br, I) *J. Comp. Chem.* **37** 2202
77. Saha R, Pan S, Mandal S, Orozco M, Merino G and Chattaraj P K 2016 Noble gas supported B_3^+ cluster: Formation of strong covalent noble gas–boron bonds *RSC Adv.* **6** 78611
78. Pan S, Ghara M, Ghosh S and Chattaraj P K 2016 Noble gas bound beryllium chromate and beryllium hydrogen phosphate: A comparison with noble gas bound beryllium oxide *RSC Adv.* **6** 92786
79. Jana G, Saha R, Pan S, Kumar A, Merino G and Chattaraj P K 2016 Noble gas binding ability of metal-bipyridine monocationic complexes (metal = Cu, Ag, Au): A computational study *ChemistrySelect* **1** 5842
80. Pan S, Moreno D, Ghosh S, Chattaraj P K and Merino G 2016 Structure and stability of noble gas bound EX_3^+ compounds (E = C, Ge, Sn, Pb; X = H, F, Cl, Br) *J. Comp. Chem.* **37** 226
81. Pan S, Gupta A, Saha R, Merino G and Chattaraj P K 2015 A coupled-cluster study on the noble gas binding ability of metal cyanides versus metal halides (metal = Cu, Ag, Au) *J. Comp. Chem.* **36** 2168
82. Pan S, Saha R and Chattaraj P K 2015 Exploring the nature of silicon-noble gas bonds in $H_3SiNgNSi$ and HSiNgNSi compounds (Ng = Xe, Rn) *Int. J. Mol. Sci.* **16** 6402
83. Pan S, Saha R and Chattaraj P K 2015 On the stability of noble gas bound 1-tris (pyrazolyl) borate beryllium and magnesium complexes *New J. Chem.* **39** 6778
84. Ghara M, Pan S, Deb J, Kumar A, Sarkar U and Chattaraj P K 2016 A computational study on structure, stability and bonding in noble gas bound metal nitrates, sulfates and carbonates (metal = Cu, Ag, Au) *J. Chem. Sci.* **128** 1537
85. Pan S, Mandal S and Chattaraj P K 2015 Cucurbit[6] uril: A possible host for noble gas atoms *J. Phys. Chem. B* **119** 10962
86. Khatua M, Pan S and Chattaraj P K 2014 Confinement induced binding of noble gas atoms *J. Chem. Phys.* **140** 164306
87. Pan S, Moreno D, Cabellos J L, Merino G and Chattaraj P K 2014 Ab initio study on the stability of $Ng_nBe_2N_2$, $Ng_nBe_3N_2$ and $NgBeSiN_2$ clusters *ChemPhysChem* **15** 2618
88. Pan S, Moreno D, Merino G and Chattaraj P K 2014 Stability of noble-gas-bound SiH_3^+ clusters *ChemPhysChem* **15** 3554
89. Khatua M, Pan S and Chattaraj P K 2014 Movement of Ng_2 molecules confined in a C_{60} cage: An ab initio molecular dynamics study *Chem. Phys. Lett.* **610** 351
90. Pan S, Contreras M, Romero J, Reyes A, Chattaraj P K and Merino G 2013 $C_5Li_7^+$ and $O_2Li_5^+$ as noble-gas-trapping agents *Chem. Eur. J.* **19** 2322
91. Pan S, Jalife S, Kumar R M, Subramanian V, Merino G and Chattaraj P K 2013 Structure and stability of $(NG)_nCN_3Be_3^+$ clusters and comparison with $(NG)BeY^{0/+}$ *ChemPhysChem* **14** 2511
92. Pan S, Jalife S, Romero J, Reyes A, Merino G and Chattaraj P K 2013 Attractive Xe–Li interaction in Li-decorated clusters *Comp. Theo. Chem.* **1021** 62
93. Zhao Y and Truhlar D G 2008 The M06 suite of density functionals for main group thermochemistry, thermochemical kinetics, noncovalent interactions, excited states, and transition elements: Two new functionals and systematic testing of four M06-class functionals and 12 other functional *Theor. Chem. Acc.* **120** 215
94. Krishnan R, Binkley J S, Seeger R and Pople J A 1980 Self-consistent molecular orbital methods. XX. A basis set for correlated wave functions *J. Chem. Phys.* **72** 650
95. Clark T, Chandrasekhar J, Spitznagel G W and Schleyer P V R 1983 Efficient diffuse function-augmented basis sets for anion calculations. III. The 3-21+G basis set for first-row elements, Li–F *J. Comp. Chem.* **4** 294
96. Frisch M J *et al*. Gaussian 09, Revision C.01, Gaussian, Inc., Wallingford CT, 2010
97. Weigend F and Ahlrichs R 2005 Balanced basis sets of split valence, triple zeta valence and quadruple zeta valence quality for H to Rn: Design and assessment of accuracy *Phys. Chem. Chem. Phys.* **7** 3297
98. Reed A E, Weinstock R B and Weinhold F 1985 Natural population analysis *J. Chem. Phys.* **83** 735
99. Wiberg K B 1968 Application of the pople-santry-segal CNDO method to the cyclopropylcarbinyl and cyclobutyl cation and to bicyclobutane *Tetrahedron* **24** 1083
100. Mitoraj M P, Michalak A and Ziegler T A 2009 A combined charge and energy decomposition scheme for bond analysis *J. Chem. Theory Comput.* **5** 962
101. Baerends E J *et al*. ADF2013.01, SCM, Theoretical Chemistry, Vrije Universiteit, Amsterdam, The Netherlands 2013
102. te Velde G, Bickelhaupt F M, Baerends E J, Guerra C F, Van Gisbergen S J A, Snijders J G and Ziegler T 2001 Chemistry with ADF *J. Comput. Chem.* **22** 931
103. Boys S F and Bernardi F 1970 The calculation of small molecular interactions by the differences of separate total energies. Some procedures with reduced errors *Mol. Phys.* **19** 553
104. Chattaraj P K and Parr R G 1993 In *Density functional theory of chemical hardness, in chemical hardness, structure and bonding* K D Sen and D M P Mingos (Eds.) Vol. 80 (Berlin: Springer-Verlag) pp. 11–25
105. Pan S, Solà M and Chattaraj P K 2013 On the validity of the maximum hardness principle and the minimum electrophilicity principle during chemical reactions *J. Phys. Chem. A* **117** 1843
106. Pan S and Chattaraj P K 2013 Favorable direction in a chemical reaction through the maximum hardness principle *J. Mex. Chem. Soc.* **57** 23
107. Saha R, Pan S and Chattaraj P K 2016 Statistical significance of the maximum hardness principle applied to some selected chemical reactions *Molecules* **21** 1477
108. Saha R, Pan S, Frenking G, Chattaraj P M and Merino G 2017 The strongest CO binding and the largest C–O stretching frequency *Phys. Chem. Chem. Phys.* doi: 10.1039/C6CP06824C
109. Barroso J, Mondal S, Cabellos J L, Osorio E, Pan S and Merino G 2017 Structure and bonding of alkali-metal pentalenides *Organometallics* doi: 10.1021/acs.organomet.6b00768

110. Mondal S, Osorio E, Pan S, Cabellos J L, Martínez S, Florez E and Merino G 2016 Why CpAl–$Cr(CO)_5$ is linear while CpIn–$Cr(CO)_5$ is not? Understanding the structure and bonding of the CpE–$Cr(CO)_5$ (E = Group 13 element) complexes *Theor. Chem. Acc.* **135** 240
111. Pan S, Saha R, Mandal S, Mondal S, Gupta A, Fernández-Herrera M A, Merino G and Chattaraj P K 2016 Selectivity in gas adsorption by molecular cucurbit[6]uril *J. Phys. Chem. C* **120** 13911
112. Mondal S, Cabellos J L, Pan S, Osorio E, Torres-Vega J J, Tiznado W, Restrepo R and Merino G 2016 10-π-Electron arenes à la carte: Structure and bonding of the [E-(C_nH_n)-E]$^{n-6}$ (E = Ca, Sr, Ba; n = 6–8) complexes *Phys. Chem. Chem. Phys.* **18** 11909
113. Liu L, Moreno D, Osorio E, Castro A C, Pan S, Chattaraj P K, Heine T and Merino G 2016 Structure and bonding of IrB_{12}^-: Converting a rigid boron B_{12} platelet to a wankel motor *RSC Adv.* **6** 27177
114. Vargas-Caamal A, Pan S, Ortiz-Chi F, Cabellos J L, Boto R A, Contreras-Garcia J, Restrepo A, Chattaraj P K and Merino G 2016 How strong are the metallocene-metallocene interactions? Cases of ferrocene, ruthenocene, and osmocene *Phys. Chem. Chem. Phys.* **18** 550